Available online at www.sciencedirect.com
ScienceDirect
Journal of Power Sources 175 (2008) 724–731
JOURNAL OF POWER SOURCES
www.elsevier.com/locate/jpowsour

Improvement of electrochemical performances of sulfonated poly(arylene ether sulfone) *via* incorporation of sulfonated poly(arylene ether benzimidazole)

Young Taik Hong [a,*], Chang Hyun Lee [b], Hyung Su Park [a,c], Kyung A. Min [b], Hyung Joong Kim [c], Sang Yong Nam [d], Young Moo Lee [b,**]

[a] *Energy Materials Research Center, Korea Research Institute of Chemical Technology, Yuseong, Daejeon 305-600, South Korea*
[b] *School of Chemical Engineering, Hanyang University, Seoul 133-791, South Korea*
[c] *Division of Advanced Materials Engineering, Kongju National University, Kongju 314-701, South Korea*
[d] *Department of Polymer Science and Engineering, Engineering Research Institute, Gyeongsang National University, Jinju 660-701, South Korea*

Received 4 July 2007; received in revised form 13 September 2007; accepted 13 September 2007
Available online 2 October 2007

Abstract

In the present study, modified acid–base blend membranes were fabricated *via* incorporation of sulfonated poly(arylene ether benzimidazole) (SPAEBI) into sulfonated poly(arylene ether sulfone) (SPAES). These membranes had excellent methanol-barrier properties in addition to an ability to compensate for the loss of proton conductivity that typically occurs in general acid–base blend system. To fabricate the membranes, SPAEBIs, which served as amphiphilic polymers with different degrees of sulfonation (0–50 mol%), were synthesized by polycondensation and added to SPAES. It resulted in the formation of acid–amphiphilic complexes such as $[PAES\text{-}SO_3]^-\ ^+[H\text{-}SPAEBI]$ through the ionic crosslinking, which prevented SO_3H groups in the complex from transporting free protons in an aqueous medium, contributing to a reduction of ion exchange capacity values and water uptake in the blend membranes, and leading to lower methanol permeability in a water–methanol mixture. Unfortunately, the ionic bonding formation was accompanied by a decrease of bound water content and proton conductivity, although the latter problem was solved to some extent by the incorporation of additional SO_3H groups in SPAEBI. In the SPAES–SPAEBI blend membranes, enhancement of proton conductivity and methanol-barrier property was prominent at temperatures over 90 °C. The direct methanol fuel cell (DMFC) performance, which was based on SPAES–SPAEBI-50–5, was 1.2 times higher than that of Nafion® 117 under the same operating condition.

Keywords: Direct methanol fuel cell; Acid–amphiphilic blend membrane; Sulfonated poly(arylene ether sulfone); Sulfonated poly(arylene ether benzimidazole)

1. Introduction

Proton exchange membrane (PEM) is one of key elements in solid typed fuel cells such as the polymer electrolyte fuel cell (PEFC) and direct methanol fuel cell (DMFC). A PEM comprises a membrane-electrode assembly (MEA) in combination with catalyst layers containing Pt or Pt–Ru alloy. High performance PEMs should satisfy many requirements including high proton conductivity and membrane durability. Because methanol transported across PEM induces catalyst poisoning and water flooding, and leads to a rapid reduction of single cell performances, fuel barrier properties are indispensable for accomplishing excellent electrochemical performances; this is particularly true of DMFC [1–4]. Nafion®, a commercially available perfluorinated sulfonic acid (PFSA) ionomer, exhibits high proton conductivity and long-term durability; however, its high methanol permeability gives rise to severe obstacles that ultimately decrease performance of the fuel cell.

Due to their high thermal stability, excellent mechanical strength, and strong resistance to membrane decomposition in

* Corresponding author. Tel.: +82 42 860 7292; fax: +82 42 861 4151.
** Corresponding author. Tel.: +82 2 2220 0525; fax: +82 2 2291 5982.
E-mail addresses: ythong@krict.re.kr (Y.T. Hong), ymlee@hanyang.ac.kr (Y.M. Lee).

0378-7753/$ – see front matter © 2007 Published by Elsevier B.V.
doi:10.1016/j.jpowsour.2007.09.068

an acidic water medium, sulfonated polyarylene ether derivatives (SPAEs) have been a focus of current investigations of alternatives to the highly methanol-permeable Nafion® membrane for DMFC applications [5–14]. SPAEs include sulfonated polysulfone [5], sulfonated poly(arylene ether ketone) [6–9], and sulfonated poly(arylene ether sulfone) [10–13]. In most cases, SPAEs are fabricated *via* direct copolymerization using aromatic diols and disulfonated/non-sulfonated aromatic halides with constant chemical compositions. The monomer sulfonation and subsequent polycondensation process has been used extensively to avoid excessive water swelling or dissolution of the resulting SPAE membranes in water after post-sulfonation of the polyarylene matrix. However, in spite of the ease in the control of the water uptake level, this method contains unsolved problems for fabricating desirable PEMs. Specifically, sufficient water uptake and preservation of this uptake within the membrane can lead to consecutive proton conduction because of a strong dependence of proton conductivity on connectivity of hydrophilic water channels. Conversely, highly sulfonated polymer membranes become both weak in mechanical strength and sensitive to hydrolytic degradation. On the other hand, sulfonated polymer membranes with low level of sulfonation exhibit strong mechanical strength and excellent membrane stability, although the membranes have undesirable proton transport properties during fuel cell operation.

Crosslinking can be a simple and powerful solution to overcome the limitations of the intrinsic properties of sulfonated aromatic polymers, and to date there have been several approaches dealing with the chemical and physical crosslinking of such polymers [15–25]. Among these approaches, there were acid–base blend systems which were composed of acidic polymer components including sulfonated polyarylenes and various basic polymer components such as poly(4-vinlypyridine), polyethylenimine (PEI), and polybenzimidazole (PBI) [24–26]. In the blend system, each component in the system was crosslinked *via* ionic interaction, resulting in a significant enhancement of membrane stability and methanol-barrier property, even under thermally and chemically harsh conditions. Unfortunately, a high degree of crosslinking caused a severe decrease in proton conductivity through PEMs, leading to a reduction of electrochemical single cell performances [24–26].

In the present study, a new approach to compensate the reduced proton conductivity shown in the typical acid–base blend systems and, thereby, to improve electrochemical performances of the resulting PEMs was addressed *via* incorporation of amphiphilic polymer instead of basic polymer. The influence of the amphiphilic polymer on overall membrane performances such as water uptake, proton conductivity, and methanol permeability was investigated with respect to its degree of sulfonation (DS) and incorporated content. For this, sulfonated poly(arylne ether sulfone) (SPAES) was fabricated as an acidic polymer, and then blended with amphiphilic sulfonated poly(arylene ether bezimidazole) (SPAEBI) which contains both sulfonic acid (–SO_3H) groups and basic benzimidazole groups. This blending was believed to result in the formation of the crosslinked polymer network derived from physical interaction of SPAES–SPAEBI and SPAEBI–SPAEBI chains, producing membranes with not only excellent methanol-barrier properties but improved dimensional stabilities. Finally, the electrochemical single cell performances of the MEAs based on the blend membranes were evaluated by comparing with Nafion® 117.

2. Experimental

2.1. Materials

4,4′-Dichlorodiphenylsulfone (DCDPS) and 4,4′-biphenol (BP) as the aromatic halide and diol, respectively, purchased from Tokyo Kasei Co. (Tokyo, Japan), were recrystallized with ethanol and dried under vacuum at 120 °C for 1 day. DCDPS was converted to 3,3′-disulfonate-4,4′-dichlorodiphenylsulfone (SDCDPS, Yield: 91.4%) using fuming sulfuric acid (28% free SO_3, Aldrich, WI, USA) [11]. Phenyl-4-hydroxybenzoate (Tokyo Kasei Co., Tokyo, Japan) and 3,3′,4,4′-tetraaminobiphenyl (Aldrich, WI, USA) were recrystallized with toluene and water with a small amount of sodiumdithionite (Aldrich, WI, USA), respectively. Bis(4-fluorodiphenyl) sulfone (DFDPS, Aldrich, WI, USA) was reacted with fuming sulfuric acid to prepare disulfonated DFDPS (SDFDPS). Toluene, potassium carbonate, dimethyl acetamide (DMAc), sodium chloride, sodium hydroxide, and diphenylsulfone were purchased from Aldrich Chemical Co. (WI, USA) and were used as received. *N*-Methylpyrrolidinone (NMP, Aldrich, WI, USA) was used as a solvent and was purified with distillation using calcium hydride at about 80 °C.

2.2. Synthesis of sulfonated poly(arylne ether sulfone) (SPAES)

Prior to the synthesis of SPAES, sulfonated 4,4′-dichlorodiphenylsulfone (SDCDPS) was exchanged in a NaCl solution to form sodium-salted SDCDPS (Na-SDCDPS) and neutralized with a small amount of NaOH. Pristine SPAES was synthesized by direct copolymerization of Na-SDCDPS (4 mmol, 3.9301 g), DCDPS (6 mmol, 3.4460 g) and BP (10 mmol, 3.7242 g) as previously reported [11,27]. The reaction mixture was stirred at ambient conditions for a few minutes and then successively refluxed at 130 °C for 3 h to remove the toluene and water by azeotropic distillation. After refluxing, the Dean–Stark trap was drained, and the reaction temperature was raised to 190 °C and maintained for a further 16 h. The resulting solution was slowly precipitated in ice water. The fiber-shaped precipitate of SPAES was collected by filtration and washed with hot water to eliminate K_2CO_3. The final SPAES powder was dried in vacuum oven at 120 °C and its inherent viscosity was about 2.02 dL g^{-1}.

IR (KBr, cm^{-1}): 1006 (diphenyl ether), 1030, 1098 (sodium sulfonate).

2.3. Synthesis of 6,6′-bis[2-(4-hydroxyphenyl) benzimidazole] (BHPB)

A three-neck flask was first charged with phenyl-4-hydroxybenzoate (0.246 mol, 52.62 g) and 3,3′,4,4′-tetraamino-

biphenyl (0.12 mol, 25.80 g), and then diphenylsulfone and toluene were added to the mixture. The mixture was heated at 150 °C under a nitrogen atmosphere for 2.5 h until no water was observed in Dean–Stark trap. Then, the reaction temperature was increased to 250 °C and maintained for a further 0.75 h. Next, the reaction was placed under vacuum and the temperature was subsequently raised to 280 °C and maintained for 1.25 h. The resulting mixture was then washed repeatedly in hot acetone and toluene, and dried in a vacuum oven at 110 °C. The mixture was recrystallized twice with DMAc using charcoal. The dark-brown 6,6′-bis[2-(4-hydroxyphenyl) benzimidazole] (BHPB) was obtained as final product (Yield: 56%, and mass: 420 Da).

IR (KBr, cm^{-1}): 3145, 3185, 3410 (benzimidazole) 3620 (OH).

^{1}H NMR spectrum (DMSO-d_6, 400 MHz, δ, ppm): 6.95–6.97 (d, 4H), 7.49–7.51 (d, 2H), 7.63–7.65 (d, 2H), 7.81 (s, 2H), 8.06–8.08 (d, 4H), 9.99 (s, 2H).

Elemental analysis ($C_{26}H_{18}N_4O_2$, 420.42 Da): Cal. C (74.28%), H (3.84%), N (6.66%), and O (15.22%), Found C (74.31%), H (3.85%), N (6.66%), and O (14.54%).

2.4. Synthesis of poly(arylene ether bezimidazole) (SPAEBI)

Before use, SDFDPS was converted into a sodium-salted form (Na-SDFDPS). A SPAEBI (Yield: 98%, ion exchange capacity (IEC) = 1.40 mequiv. g^{-1}) was synthesized using Na-SDFDPS (5 mmol, 2.29 g), DFDPS (5 mmol, 1.27 g) and BHPB (10 mmol, 4.2 g) based on the procedure shown in Scheme 1. A series of analogous copolymers were prepared by decreasing the mole ratio of SDFDPS (40, 30, 20, and 0 mol%, respectively) to total halide monomers.

IR (KBr, cm^{-1}): 1030, 1097 (sodium sulfonate) 3145, 3184, 3410 (benzimidazole).

^{1}H NMR spectrum (DMSO-d_6) was shown in Fig. 1.

2.5. Fabrication of SPAES–SPAEBI blend membrane

Different amounts of SPAEBI (0, 3, 5, 10, and 15 wt.%) were re-dissolved in NMP and blended with SPAES (DS = 40%) solution by a mechanical stirring for 1 day. After casting each solution (∼15 wt.%) onto glass plate, it was slightly dried at 60 °C for 8 h and heated at 120 °C for 8 h in vacuum oven. The resulting SPAES–SPAEBI blend membranes were obtained in a salted sulfonated form. The nominal thickness of all the membranes was approximately 30–70 μm. The membranes were acidified by boiling them in a 1 M H_2SO_4 solution for 1 day and were then washed thoroughly with deionized water. Finally, semi-transparent brown colored polymer blend membranes were obtained. In the nomenclature of each membrane (SPAES–SPAEBI-#$_1$–#$_2$), #$_1$ and #$_2$ indicate mol% of SDFDPS in SPAEBI and amount of SPAEBI (wt.%) in the blend system, respectively. For example, SPAES–SPAEBI-50–5 represents the blend of a SPAES (DS = 40%) and a 5 wt.% SPAEBI which has 50 mol% of SDFDPS.

2.6. Evaluation of the SPAES–SPAEBI blend membranes

Spectroscopic analyses of the SPAES–SPAEBI blend membranes were carried out using a Fourier transform infrared spectrometer (FT-IR, Nicolet Magna IR 76 spectrometer, Madison, WI, USA) and a ^{1}H nuclear magnetic resonance spectroscopy (NMR, Varian model NMR 1000, CA, USA). In addition, synthesis of the BHPB monomer was confirmed by elemental analysis (EA, Model EA 1108, Carlo Erba Instru-

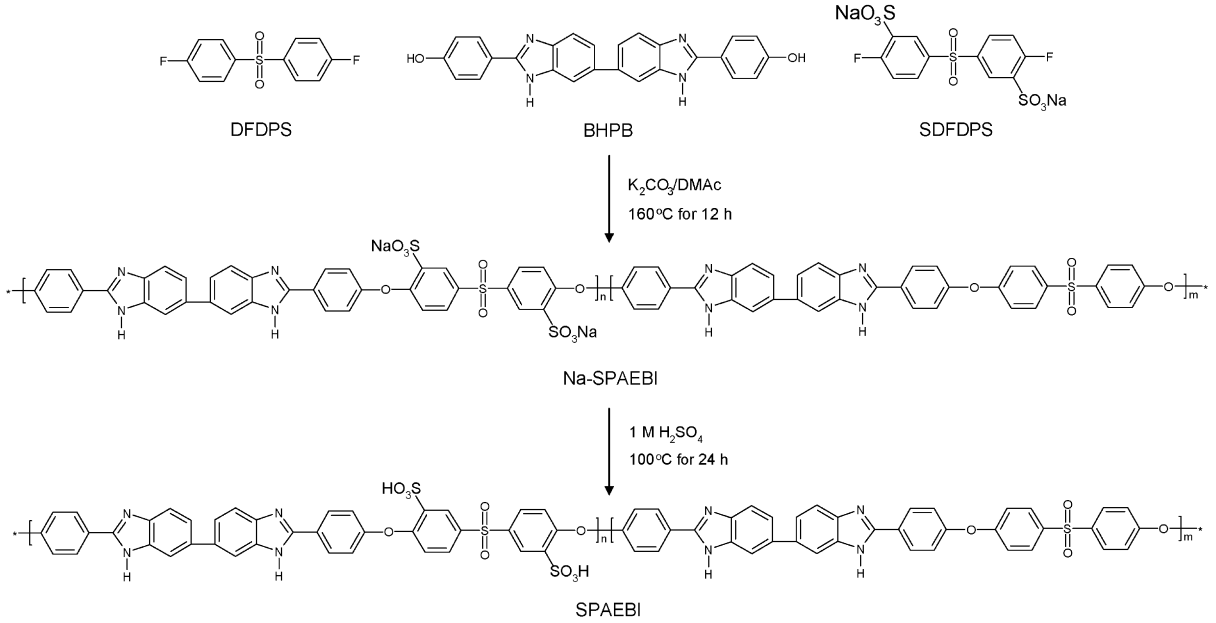

Scheme 1. Synthetic scheme of sulfonated poly(arylene ether benzimidazole) (SPAEBI).

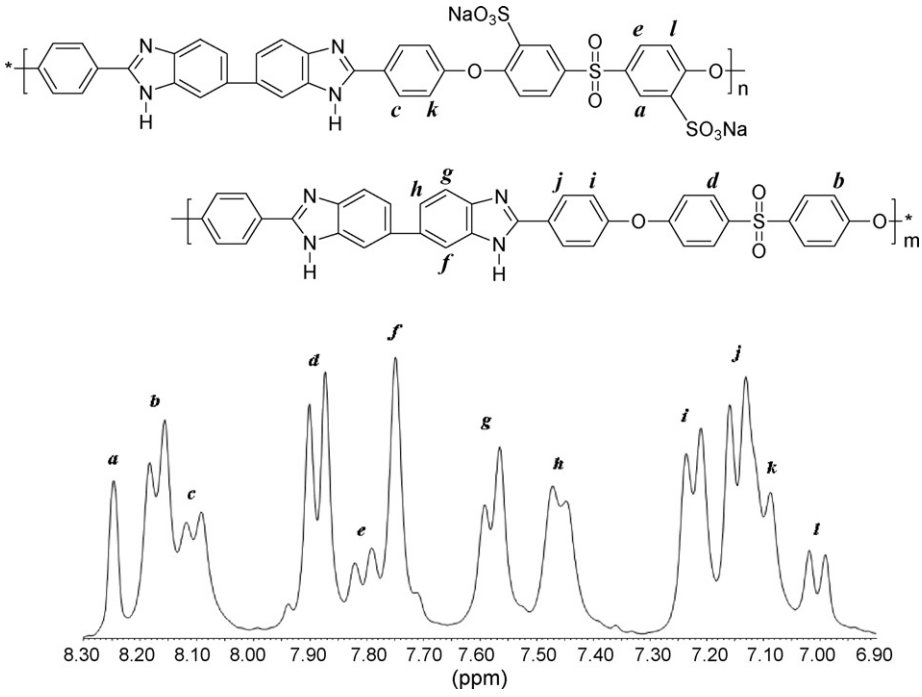

Fig. 1. ^{1}H NMR spectrum of sulfonated poly(arylene ether benzimidazole) (SPAEBI).

ment, Milan, Italy). The thermal decomposition processes of the blend membranes were characterized using a thermogravimetric analyzer (TGA 2050, TA instrument, New Castle, DE, USA) under an air atmosphere at a heating rate of 10 °C min^{-1} in a range of 50 to 700 °C. The ion exchange capacity (IEC, mequiv. g^{-1}) of the blend membranes was measured using a conventional titration method (ASTM D2187). The water uptake was determined by weighing the difference between a dry sample and water-swollen sample made by immersing the membrane in deionized water at 30 °C for at least 1 day. The state of water in the fully hydrated membrane was assessed using differential scanning calorimetry as previously reported (DSC, DSC 2010 thermal analyzer, TA instrument, New Castle, DE, USA) [22]. The content of free water (%) to total water uptake in each membrane sample was calculated using the equation of free water = E_{fs}/E_{Fw} × total water uptake (E_{fs}: fusion enthalpy of endothermic peak area from 0 to 10 °C and E_{Fw}: endothermic heat of fusion for pure water, 335 J g^{-1}).

The content of bound water, which was expressed as a percentage, was also obtained by calculating the difference between total water uptake and free water content. The ohmic resistance (R, Ω) of each membrane sample (dimension: 1 cm × 4 cm) was measured in liquid water at 30 °C with a four-point probe alternating current (ac) impedance spectroscopic method using both an electrode system connected with an impedance/gain phase analyzer (Solatron 1260) and an electrochemical interface (Solatron 1287, Farnborough Hampshire, ONR, UK) [28]. Measurements were performed in a shielded thermo- and hygro-controlled chamber in an electronic noise free state. Ohmic resistance was converted to proton conductivity (σ, S cm^{-1}) by means of the equation $\sigma = l/(RS)$, where l is the distance between reference electrodes and S is the cross-sectional area of membrane sample. The methanol permeability (P_{MeOH}, cm^2 s^{-1}) of the membranes was determined in an isothermal bath from 25 to 90 °C using a two chamber-diffusion cell method with a 3 M (∼6 wt.%) CH_3OH solution [19–23]. The methanol concentration gradient was periodically measured using a gas chromatography (GC, Shimadtzu, GC-14B, Tokyo, Japan) equipped with a thermal conductivity detector (TCD). Determination of the hydrolytic durability of the membranes was achieved by measuring the change of proton conductivity after immersion in liquid water at 80 °C [20–23]. The dimensional stability (initial size in dry state: 2 cm × 2 cm) of the membranes was assessed by measuring the volumetric change in the samples after they were dried at 100 °C and swollen in liquid water at 30 °C for 1 day. Measurements were repeated at least five times to ensure good reproducibility of the results.

2.7. Single cell performances of SPAES–SPAEBI blend membranes

A 5 wt.% Nafion® solution (EW = 1100, DuPont) and a Pt black (Johnson Matthey, HiSPEC 1000) for cathode were mixed in 100 ml of isopropyl alcohol in a beaker. The mixture was sonicated for 1 h to obtain well-dispersed catalyst slurry, and was then sprayed on one side of the SPAES–SPAEBI membranes at ambient temperature. The cathode catalyst-coated membranes were dried at 60 °C in vacuum oven, and the catalyst slurry containing Pt–Ru black (Johnson Matthey, HiSPEC 6000) for anode was subsequently sprayed on the other side of the membranes. The Pt and Pt–Ru loading on each electrode was 3 mg cm^{-2}.

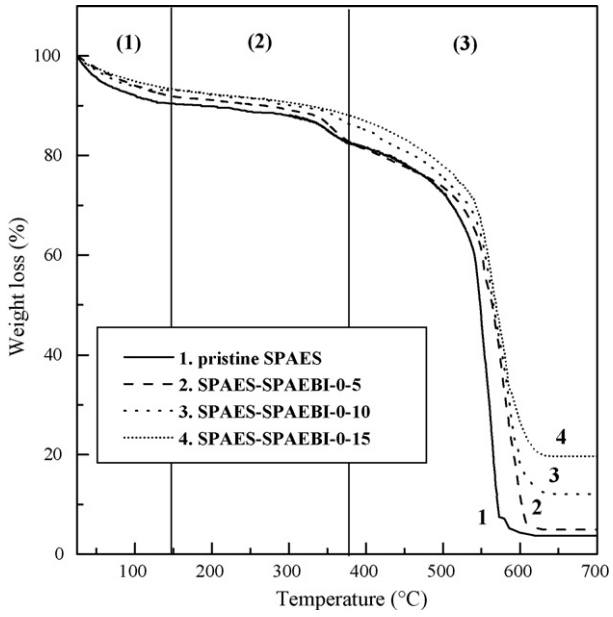

Fig. 2. TGA diagrams of pristine SPAES (1, solid), SPAES–SPAEBI-0–5 (2, dash), SPAES–SPAEBI-0–10 (3, dot), and SPAES-SPEBI-0–15 (4, solid dot).

3. Results and discussion

3.1. Thermal stability

The thermal degradation behavior of the SPAES–SPAEBI blend membranes was verified by the physical crosslinking *via* ionic interaction between strong acid (–SO_3H) and strong base (benzimidazole). Fig. 2 shows three consecutive thermal decomposition processes; (1) the thermal evaporation of water molecules below 150 °C, (2) the thermal decomposition of SO_3H groups from 150 to 375 °C, and (3) the thermal oxidation of polymer main chain over 375 °C. Incorporation of SPAEBI into pristine SPAES lowered water uptake levels in the resulting membranes and, thereby, reduced the percentage of weight loss derived from water evaporation in TGA thermogram shown in Fig. 2. This trend was distinctly observable in the blend system containing high amount of benzimidazole. Furthermore, the blending gave rise to a strong interaction between the SO_3H in SPAES and benzimidazole groups in SPAEBI, which retarded the thermal desulfonation process up to approximately 375 °C. It indicates that physical crosslinking *via* acid–amphiphilic polymer blending enhanced thermal stability of the resulting membranes.

3.2. Water uptake behavior

In hydrated membranes, proton and methanol transport behaviors are strongly dependent on water uptake and the state of water within the membranes [3,13,20–23]. Considering its high relevance with water uptake behavior, IEC should be primarily observed as an indicator of proton-releasing capability. As shown in Table 1, physical crosslinking between the Brønsted acid and base groups in the SPAES–SPAEBI-0 series (0% of SDFDPS in SPAEBI) prevented SO_3H groups in SPAES from transporting protons in a water medium. Consequently, the IEC values and water uptake of SPAES–SPAEBI-0 series decreased with a high content of the basic polymer. This trend was also observed for other SPAES–SPAEBI series membranes. Further the addition of SPAEBI with a constant sulfonation level enhanced the degree of crosslinking, rather than overall content of fixed-charged ions, i.e. SO_3H group, in the resulting blend membranes. It lowered their IEC and water uptake, leading to the improvement of dimensional stability. In contrast, the loss of IEC values in the blend membranes was compensated by the addition of SO_3H groups in SPAEBI. In SPAES–SPAEBI membranes with a constant amount of SPAEBI, a high degree of sulfonation of the amphiphilic polymer led to an increase of IEC, thus increasing water uptake.

Moreover, the physical crosslinking by ionic bonding affected the state of water within the blend membranes, which was classified as either free water or bound water. In particular, bound water is a result of a strong interaction between water molecules and ionic groups, including SO_3H groups, in polymer matrix and is significantly responsible for proton transport [3,5,13,17–23]. After incorporation of SPAEBI, the bound water content of the membranes decreased relative to that of pristine SPAES. A higher blending content of SPAEBI led to lower

Table 1
Water uptake behavior of SPAES–SPAEBI blend membranes

Types of membrane	Ion exchange capacity (mequiv. g^{-1})	Water uptake (%)	Free water (%)	Bound water (%)	Dimensional stability (%)
Pristine SPAES	1.62	62.3	36.5	63.5	63.4
SPAES–SPAEBI-0–3	1.51	57.2	42.6	57.4	58.1
SPAES–SPAEBI-0–5	1.33	52.6	46.3	53.7	48.5
SPAES–SPAEBI-0–10	1.12	38.1	56.3	43.7	22.4
SPAES–SPAEBI-0–15	0.99	31.3	65.1	34.9	13.2
SPAES–SPAEBI-20–10	1.17	39.3	54.7	45.3	24.3
SPAES–SPAEBI-30–5	1.46	55.6	44.8	55.2	54.2
SPAES–SPAEBI-30–10	1.22	41.2	52.5	47.5	26.7
SPAES–SPAEBI-30–15	1.04	32.6	62.4	37.6	17.1
SPAES–SPAEBI-40–10	1.27	42.4	50.3	49.7	29.3
SPAES–SPAEBI-50–5	1.55	58.2	39.4	60.6	60.2
SPAES–SPAEBI-50–10	1.30	43.1	48.2	51.8	32.5
SPAES–SPAEBI-50–15	1.10	36.4	59.1	40.9	20.5

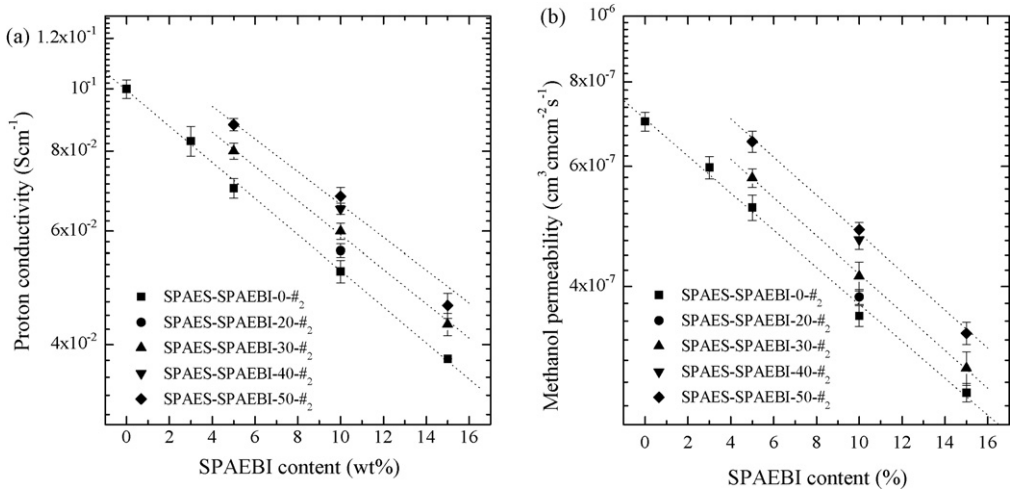

Fig. 3. Relationship between (a) proton conductivity and (b) methanol permeability of the various membranes with respective to content and varying degree of sulfonation of SPAEBI. Proton conductivity and methanol permeability of each membrane were measured in liquid water and 3 M methanol–water mixture at 25 °C, respectively.

bound water content in the resulting membranes. It means that the acid–amphiphilic complex ($[PAES\text{-}SO_3]^-$ $^+$[H-SPAEBI]) was intensified when the incorporated content of SPAEBI was high, which prohibited water molecules from forming a strong interaction with SO_3H groups in the blend system. However, a reduction of bound water was balanced to some extent by an increase of sulfonation level of SPAEBI. As a result, the SPAES–SPAEBI-50–5 with a high DS and a low blending content showed high bound water content similar to pristine SPAES.

3.3. Proton conductivity and methanol permeability

The correlation of proton and methanol transport behavior through SPAES–SPAEBI blend membrane in the hydrate state is shown in Fig. 3. According to the vehicle mechanism, protons can combine with water and methanol molecules to form cationic complexes such as H_3O^+, $H_5O_2^+$, $H_9H_4^+$, and $CH_3OH_2^+$ [29–32]. After formation, the complexes permeate through localized hydrophilic water channels within PEMs. Therefore, most PEMs with high proton conductivity are highly permeable to methanol molecules, while low proton-conductive membranes exhibit a low permeability to methanol. This correlation was also observed for SPAES–SPAEBI blend membranes. Incorporation of SPAEBI into pristine SPAES membrane resulted in relatively low water swelling and improved methanol-barrier properties. This blending simultaneously reduced the non-volatile bound water content of the resulting membranes and lowered their proton conductivities. On the other hand, incorporation of an amphiphilic polymer with a high sulfonation level contributed to the enhancement of proton conductivity, even in a small blending content. Unfortunately, the addition of SO_3H groups to SPAEBI was accompanied by an increase in methanol permeability, indicating that blending with amphiphilic polymers was not an omnipotent method able to improve both proton conductivity and methanol-barrier property at low temperatures.

The proton and methanol transport behavior at elevated temperatures from 25 to 90 °C is shown in Fig. 4. Among the blend membranes, SPAES–SPAEBI-50–5, which had the highest proton conductivity, was selected for the purpose of observing the relationship between transport properties and temperature relative to pristine SPAES and Nafion® 117 as a standard membrane for DMFC application. The elevation of the measuring temperature in the incorporation system altered the proton and methanol transport properties in each membrane. The proton conductivity of each membrane in liquid water increased successively with increasing temperatures. Irrespective of polymer types, a very similar activation energy (5.06–5.22 kcal mol^{-1} K^{-1}) was obtained. The methanol diffusion through each membrane was also accelerated by temperature. Interestingly, in spite of the methanol permeability similar to that of pristine SPAES at 25 °C, SPAES–SPAEBI-50–5 exhibited higher methanol-barrier properties than non-crosslinked polymer membranes such as pristine SPAES and Nafion® 117 at higher temperatures. This finding

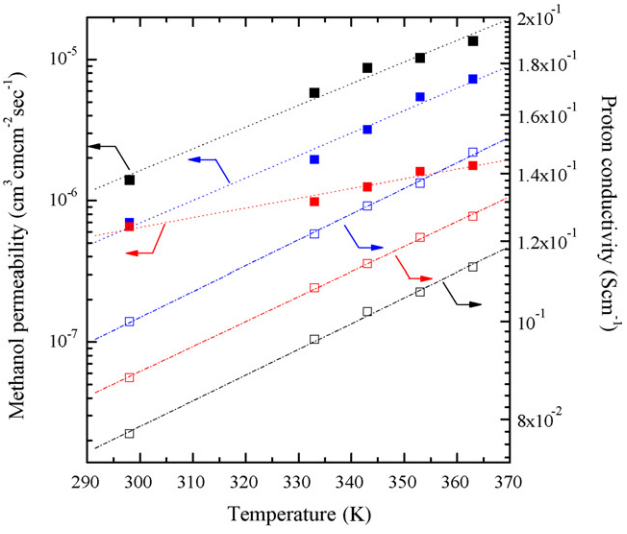

Fig. 4. Temperature dependence of proton conductivity (left side) and methanol permeability (right side) of pristine SPAES (blue), SPAES–SPAEBI-50–5 (red), and Nafion® 117 (black).

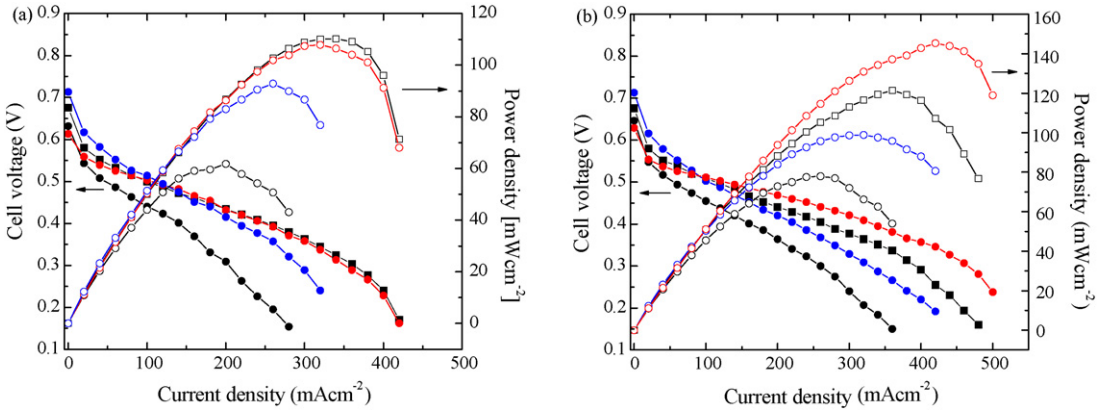

Fig. 5. Single cell performances of Nafion® 117 (square) and SPAES derivatives (circle) including pristine SPAES (black), SPAES–SPAEBI-50–10 (blue), and SPAES–SPAEBI-50–5 (red) at (a) 80 °C and (b) 90 °C under a 3 M MeOH 1 cm^3 min^{-1} and O_2 200 cm^3 min^{-1} condition.

suggests that the effect of physical crosslinking on the suppression of methanol transport across SPAES–SPAEBI membranes was conspicuous at high temperatures rather than at low temperatures. Considering the improved proton conductivity and methanol suppression at elevated temperatures, the application of SPAES–SPAEBI blend membranes may be useful in DMFC system operated at relatively high temperatures (above 80 °C).

3.4. Single cell performances

In general, high proton conductivity and low methanol permeability are inevitably required to guarantee excellent DMFC performance [33–36]. Differing from MEAs based on PFSA membranes, high contact resistance is observed between non-perfluorinated membranes and Nafion® ionomer as a catalyst binder for proton migration in catalyst layers. This is attributable to a large difference in the swelling ratio of the heterogeneous polymers in a water–methanol mixture. Consequently, the single cell performances of these types of MEA decrease rapidly within a short time [37].

The electrochemical single cell performances of SPAES–SPAEBI blend membranes using a 3 M methanol solution under different DMFC operation temperatures are shown in Fig. 5. Nafion® 117 and pristine SPAES were used for comparison. Complicating factors, such as proton conductivity, methanol permeability and contact resistance, influenced the electrochemical properties of the SPAES–SPAEBI blend membranes. Physical crosslinking with SPAEBI reduced methanol crossover relative to pristine SPAES, contributing to an enhancement of single cell performances in the SPAES–SPAEBI blend membranes. SPAES–SPAEBI-50–5 with high proton conductivity displayed a higher electrochemical performance than SPAES–SPAES-50–10 with low methanol permeability. This finding indicated that the effect of proton conductivity on DMFC performances, rather than that of methanol permeability, was predominant at low concentrations of methanol (below 3 M). This result was consistent with previous findings [34,35,38,39]. In spite of a higher proton conductivity and lower methanol permeability, the DMFC performance of SPAES–SPAEBI-50–5 was similar to, or somewhat lower than, Nafion® 117 at 80 °C (Fig. 5(a)). This may have been due to a relatively weak adhesion between SPAES–SPAEBI-50–5 and catalyst layers containing the Nafion® binder.

Differences in methanol permeability and proton conductivity of SPAES–SPAEBI-50–5 and Nafion® 117 became larger as the temperatures were higher than 90 °C, which allowed the MEA based on SPAES–SPAEBI-50–5 to overcome the potential loss resulting from the adhesion problems with catalyst layers. Indeed, the SPAES–SPAEBI-50–5 exhibited an outstanding DMFC performance (330 mA cm^{-2} at 0.4 V and maximum power density = 145 mW cm^{-2} at 0.3 V), which was superior to Nafion® 117 (270 mA cm^{-2} at 0.4 V and maximum power density = 121 mW cm^{-2} at 0.3 V) at 90 °C in Fig. 5(b). Although it is well known that most of hydrocarbon membranes do not have good stability in acid environment, we never find big electrochemical performance drops in relation to membrane decomposition during a short term DMFC operation of 100 h. It is noted that adding constant amount of sulfonated poly(arylene ether benzimidazole) into sulfonated poly(arylene ether sulfone) polymer matrix caused physical crosslinking, thus improving membrane durability even in acid environment. Presently, we plan to focus on long-term DMFC operation over 90 °C using the SPAES–SPAEBI-50–5 and development of custom-tailored binder materials appropriate for SPAES derivatives. We will report the relation between membrane durability and long-term fuel cell performance, even being operated with higher methanol concentrations in near future.

4. Conclusions

The amphiphilic polymers were incorporated into an acidic polymer to make up for the reduction of proton conductivity observed in the general acid–base blend systems and thereby to improve their electrochemical performances. Due to the incorporation, the ionic bonding between the SO_3H groups in SPAES and benzimidazole groups in SPAEBI formed an acid–amphiphilic complex, $[PAES\text{-}SO_3]^- {}^+[H\text{-}SPAEBI]$. Consequently, it was found that the physical crosslinking between acidic SPAES and amphiphilic SPAEBI was effective enough to

reduce IEC values and water uptake, thus improving methanol suppression through SPAES–SPAEBI blend membranes as well as dimensional stability. Nonetheless, undesirable loss of proton conductivity occurred, even in acid–amphiphilic membranes. This trend was obviously observed for the blend membranes with high incorporated content of SPAEBI.

The reduction of proton conductivity that occurred after blending with basic polymers was compensated by increasing the degree of sulfonation of SPAEBI, although this subsequently weakened their methanol-barrier properties. However, the elevation of temperature altered both the proton and methanol transport behavior of SPAES–SPAEBI blend membranes with physically crosslinked microstructures. The methanol permeability of SPAES–SPAEBI membranes increased slowly at elevated temperatures, while their proton conductivity increased with a similar increment to those of non-crosslinked membranes such as pristine SPAES and Nafion® 117. Consequently, the difference in methanol permeability between SPAES–SPAEBI and other membranes became large at the elevated temperatures. In DMFC application over 90 °C, SPAES–SPAEBI blend membranes, which had excellent proton conductivity and methanol suppression capability, exhibited outstanding single cell performances compared with those of pristine SPAES and Nafion® 117. It will be useful to develop available PEMs for DMFC using the acid–amphiphilic polymer blend system investigated in the present study.

Acknowledgement

The authors would like to thank the Ministry of Commerce, Industry, and Energy for funding this research.

References

[1] A. Heinzel, V.M. Barragam, J. Power Sources 84 (1999) 70–74.
[2] X. Ren, P. Zelenay, S. Thomas, J. Davey, S. Gottesfeld, J. Power Sources 86 (2001) 111–116.
[3] K. Nagai, Y.M. Lee, T. Masuda, in: K. Matyjaszewski, Y. Gnanou, L. Leibler (Eds.), Macromolecular Engineering: Precise Synthesis, Materials Properties, Application, vol. 4, Wiley–VCH, Weinheim, 2007, pp. 2451–2492.
[4] G.Q. Lu, C.Y. Wang, J. Power Sources 134 (2004) 33–40.
[5] H.B. Park, H.S. Shin, Y.M. Lee, J.W. Rhim, J. Membr. Sci. 247 (2005) 103–110.
[6] M. Gil, X. Ji, X. Li, H. Na, J.E. Hampsey, Y. Lu, J. Membr. Sci. 234 (2004) 75–81.
[7] X. Shang, X. Li, M. Xiao, Y. Meng, Polymer 47 (2006) 3807–3813.
[8] F. Wang, T. Chen, J. Xu, T. Liu, H. Jiang, Y. Qi, S. Liu, X. Li, Polymer 47 (2006) 4148–4153.
[9] Y. Gao, G.P. Robertson, M.D. Guiver, G. Wang, X. Jian, S.D. Mikhailenko, X. Li, S. Kaliaguine, J. Membr. Sci. 278 (2006) 26–34.
[10] Y. Li, F. Wang, J. Yang, D. Liu, A. Roy, S. Case, J. Lesko, J.E. McGrath, Polymer 47 (2006) 4210–4217.
[11] F. Wang, M. Hickner, Y.S. Kim, T.A. Zawodzinski, J.E. McGrath, J. Membr. Sci. 197 (2002) 231–242.
[12] Y.S. Kim, B. Einsla, M. Sankir, W. Harrison, B.S. Pivovar, Polymer 47 (2006) 4026–4035.
[13] D.S. Kim, K.H. Shin, H.B. Park, Y.S. Chung, S.Y. Nam, Y.M. Lee, J. Membr. Sci. 278 (2006) 428–436.
[14] H. Ghassemi, J.E. McGrath, T.A. Zawodzinski, Polymer 47 (2006) 4132–4139.
[15] P. Xing, G.P. Robertson, M.D. Guiver, S.D. Mikhailenko, K. Wang, S. Kaliaguine, J. Membr. Sci. 229 (2004) 95–106.
[16] S.D. Mikhailenko, K. Wang, S. Kaliaguine, P. Xing, G.P. Robertson, M.D. Guiver, J. Membr. Sci. 233 (2004) 93–99.
[17] J.W. Rhim, H.B. Park, C.S. Lee, J.H. Jun, D.S. Kim, Y.M. Lee, J. Membr. Sci. 238 (2004) 143–151.
[18] D.S. Kim, H.B. Park, J.W. Rhim, Y.M. Lee, J. Membr. Sci. 240 (2004) 37–48.
[19] Y.M. Lee, H.B. Park, C.H. Lee, US 7,157,548 B2 (2007).
[20] H.B. Park, C.H. Lee, Y.M. Lee, B.D. Freeman, H.J. Kim, J. Membr. Sci. 285 (2006) 432–443.
[21] C.H. Lee, H.B. Park, Y.S. Chung, Y.M. Lee, B.D. Freeman, Macromolecules 39 (2006) 755–764.
[22] C.H. Lee, S.Y. Hwang, C.H. Park, H.B. Park, J.Y. Kim, Y.M. Lee, Nat. Mater., in preparation.
[23] C.H. Lee, S.Y. Hwang, J.Y. Sohn, H.B. Park, J.Y. Kim, Y.M. Lee, J. Power Sources 163 (2006) 339–348.
[24] J. Kerres, A. Ullrich, F. Meier, T. Häring, Solid State Ionics 125 (1999) 243–249.
[25] J. Kerres, W. Zhang, A. Ullrich, C.M. Tang, M. Hein, V. Gogel, T. Frey, L. Jörissen, Desalination 147 (2002) 173–178.
[26] C. Hasiotis, V. Deimede, C. Kontoyannis, Electrochim. Acta 46 (2001) 2401–2406.
[27] M.J. Sumner, W.L. Harrison, R.M. Weyers, Y.S. Kim, J.E. McGrath, J.S. Riffle, A. Brink, M.H. Brink, J. Membr. Sci. 239 (2004) 199–211.
[28] C.H. Lee, H.B. Park, Y.M. Lee, R.D. Lee, Ind. Eng. Chem. Res. 44 (2005) 7617–7626.
[29] K.D. Kreuer, J. Membr. Sci. 185 (2001) 29–39.
[30] A.A. Kornyshev, A.M. Kuznetsov, E. Spohr, J. Ulstrup, J. Phys. Chem. B 107 (2003) 3351–3366.
[31] E. Spohr, P. Commer, A.A. Kornyshev, J. Phys. Chem. B 106 (2002) 10560–10569.
[32] M. Eikerling, A.A. Kornyshev, A.M. Kuznetsov, J. Ulstrup, S. Walbran, J. Phys. Chem. B 105 (2001) 3646–3662.
[33] Y.H. Su, Y.L. Liu, Y.M. Sun, J.Y. Lai, M.D. Guiver, Y. Gao, J. Power Sources 155 (2006) 111–117.
[34] J. Ge, H. Liu, J. Power Sources 142 (2005) 56–69.
[35] H. Dohle, J. Divisek, R. Jung, J. Power Sources 86 (2000) 469–477.
[36] D.W. Jung, C.H. Lee, C.S. Kim, D.R. Shin, J. Power Sources 71 (1998) 169–173.
[37] H.Y. Jung, K.Y. Cho, K.A. Sung, W.K. Kim, J.K. Park, J. Power Sources 163 (2006) 56–59.
[38] Y. Yin, O. Yamada, K. Tanaka, K. Okamoto, Polymer J. 38 (2006) 197–219.
[39] K. Scott, W.M. Taama, P. Argyropoulos, K. Sundmacher, J. Power Sources 83 (1999) 204–216.